THE JOURNAL OF BIOLOGICAL CHEMISTRY
Vol. 279, No. 32, Issue of August 6, pp. 33438–33446, 2004

Printed in U.S.A.

Functional Domain and Motif Analyses of Androgen Receptor Coregulator ARA70 and Its Differential Expression in Prostate Cancer*

Received for publication, February 18, 2004, and in revised form, May 26, 2004
Published, JBC Papers in Press, May 27, 2004, DOI 10.1074/jbc.M401781200

Yueh-Chiang Hu‡§, Shuyuan Yeh‡§, Shauh-Der Yeh‡¶, Erik R. Sampson‡, Jiaoti Huang‡, Peng Li‖, Cheng-Lung Hsu‡, Huei-Ju Ting‡, Hui-Kuan Lin‡, Liang Wang‡, Eungseok Kim‡, Jing Ni‡, and Chawnshang Chang‡

From the ‡George Whipple Laboratory for Cancer Research, Departments of Pathology, Urology, and Radiation Oncology and The Cancer Center, University of Rochester, Rochester, New York 14642, the ‖Department of Pathology, University of Texas M. D. Anderson Cancer Center, Houston, Texas 77030 and the ¶Department of Urology, Taipei Medical University, Taipei 105, Taiwan

Androgen receptor (AR)-associated coregulator 70 (ARA70) was the first identified AR coregulator. However, its molecular mechanism and biological relevance to prostate cancer remain unclear. Here we show that ARA70 interacts with and promotes AR activity via the consensus F*XX*LF motif within the ARA70-N2 domain (amino acids 176–401). However, it does not promote AR activity via the classic L*XX*LL motif located at amino acids 92–96, although this classic L*XX*LL motif is important for ARA70 to interact with other receptors, such as PPARγ. The molecular mechanisms by which ARA70 enhances AR transactivation involve the increase of AR expression, protein stability, and nuclear translocation. Furthermore, ARA70 protein is more frequently detected in prostate cancer specimens (91.74%) than in benign tissues (64.64%, $p < 0.0001$). ARA70 expression is also increased in high-grade prostate cancer tissues as well as the hormone-refractory LNCaP xenografts and prostate cancer cell lines. Because ARA70 can promote the antiandrogen hydroxyflutamide (HF)-enhanced AR transactivation, the increased ARA70 expression in hormone-refractory prostate tumors may confer the development of HF withdrawal syndrome, commonly diagnosed in patients with the later stages of prostate cancer. Because ARA70-N2 containing the AR-interacting F*XX*LF motif without coactivation function can suppress HF-enhanced AR transactivation in the hormone-refractory LNCaP cells, using the ARA70-N2 inhibitory peptide at the hormone refractory stage to battle the HF withdrawal syndrome may become an alternative strategy to treat prostate cancer.

The androgen receptor (AR)[1] is a ligand-dependent transcription factor that belongs to the steroid receptor (SR) superfamily (1, 2). Although several studies have revealed how SRs can recognize and interact with their hormone response elements (3, 4), the mechanism of how SRs activate target gene expression is not fully understood. Ligand-unbound SRs have been found in the cytosol associated with heat shock proteins (HSPs), including HSP90, HSP70, and HSP56 (5–7). Studies of the HSP chaperone machinery in eukaryotes have suggested that HSPs function to prevent SR misfolding and aggregation and promote refolding or recycling of denatured polypeptides (8, 9). It has also been reported that HSP90 may enhance the ligand binding capacity of the AR, but not the glucocorticoid receptor (10). The detailed mechanism of how these cytosolic proteins regulate SR function, however, remains to be elucidated.

Recently, it has been reported that several SRs can interact directly with components of the basal transcription machinery, such as TBP (11), TFIIB (12), TFIIF (13), and TFIIH (14). In addition, specific sets of proteins are recruited by the SRs as coregulators that may function as bridging factors between the receptors and general transcription machinery in the preinitiation complex (15, 16). Identifying and studying the function of individual components of these complexes are crucial for understanding how SRs regulate their target genes. Several coregulators including ARA70 (17), ARA55 (18), ARA54 (19), ARA160 (20), ARA24 (21), SRC-1 (22), GRIP1/TIF2 (23, 24), RAC3/ACTR/AIB1/pCIP/SRC-3 (25–28), CBP/p300 (29), and the tumor suppressors BRCA1 and Rb (30, 31), have been identified as being able to modulate the transactivation of SRs. Furthermore, the studies of coregulators have also linked the transcriptional activation of SRs to chromatin acetylation. Some of these coregulators, such as RAC3/ACTR (25–28), CBP/p300 (32), and SRC-1 (33), have been found to either have intrinsic histone acetyltransferase activity or have the capacity to recruit the p300/CBP-associated factor (p/CAF) that has histone acetyltransferase activity. The physiological significance of these coregulators and their involvement in development, differentiation, and diseases, however, remain to be further studied.

In previous reports, our results indicated that ARA70 can potentiate AR transactivation in the presence of androgen (17) and can also enhance the androgenic activity of antiandrogens or 17β-estradiol (E2) on AR (34–36). The E2-enhanced AR transactivation was further confirmed by several laboratories using different cells, such as CV-1 and HeLa (37–40). Other studies also indicated that ARA70 can enhance significantly the AR transactivation in CV-1 cells and that the expression of

* This work was supported by National Institutes of Health Grants DK067686 and DK60905 and the George H. Whipple Professorship Endowment. The costs of publication of this article were defrayed in part by the payment of page charges. This article must therefore be hereby marked "*advertisement*" in accordance with 18 U.S.C. Section 1734 solely to indicate this fact.

§ Both authors contributed equally to this work.
** To whom correspondence should be addressed. E-mail: chang@urmc.rochester.edu; Web site: www.urmc.rochester.edu/ ChangARLab.

[1] The abbreviations used are: AR, androgen receptor; ARA70, androgen receptor-associated coregulator 70; CSS, charcoal dextran-stripped serum; HF, hydroxyflutamide; HSP, heat shock protein; DBD, DNA binding domain; LBD, ligand binding domain; PPARγ, peroxisome proliferator-activated receptor; DHT, dihydrotestosterone; SR, steroid receptor; FCS, fetal calf serum; DAPI, 4′,6-diamidino-2-phenylindole.

ARA70 could be enhanced in the absence of androgen in the human prostate cancer xenograft, CWR22 (41, 42). In addition, resveratrol, a growth inhibitor for prostate cancer LNCaP cells, could repress the expression of ARA70 and the AR transactivation (43). Diminishing the ARA70 function by dominant-negative ARA70 or ARA70-specific siRNA could suppress prostate cancer cell growth (44). These results suggest that ARA70 may be an important coregulator for AR function in prostate cancer. Therefore, it is plausible that ARA70 can be a therapeutic target for prostate cancer treatment.

In the present study, we further dissect the mechanisms by which ARA70 functions as a coregulator of AR transactivation and elucidate the biological relevance between ARA70 and prostate cancer progression. Finally, we have found that ARA70-N2, which contains the AR-interacting domain, can function as an inhibitor to repress androgen- and HF-induced AR transactivation by inhibiting AR interaction with other coregulators and blockade of the AR N-/C-terminal interaction. This suggests a potential therapeutic strategy against prostate cancer.

EXPERIMENTAL PROCEDURES

Plasmids—Construction of pCMX-VP16-AR (amino acids 38~919), pCDNA3-FLAG-AR-N, and -D-L, pCMX-GAL4-PPARγ and -ARLBD, and pSG5-AR, -ARA70N, -ARA70-FL, -ARA70N-A*XX*LF, and -ARA70-N-F*XX*AA were described previously (17, 36, 45, 46). pCDNA3-FLAG-ARA70-N1 and -N2 were constructed by insertion of PCR-generated cDNAs into pCDNA3 vector (Invitrogen). The pCMX-VP16-ARA70N-L*XX*LL, pSG5-ARA70-L*XX*AA, and pSG5-ARA70N-L*XX*AA mutants were generated by two-way PCR using the following four primers: 5′-CCGGAATTCTCAGTCCACCCAAGGTCT-3′, 5′-GCTCTACTCGGCAGCGGGCCAGTTCAATTG-3′, 5′-GAACTGGCCCGCTGCCGAGTAGAGCGCTG-3′, and 5′-CGCGGATCCCTCTACCTTACATGGGTC-3′. All constructs were verified by DNA sequencing.

Cell Culture and Transfections—Human prostate cancer DU145 and PC-3 cells were maintained in Dulbecco's minimum essential medium containing penicillin (25 unit/ml), streptomycin (25 μg/ml), and 5% fetal calf serum (FCS). Androgen-responsive LNCaP prostate cancer cells were maintained in RPMI 1640 containing penicillin (25 units/ml), streptomycin (25 μg/ml), and 10% FCS. Transfections were performed using SuperFect reagent (Qiagen) according to the manufacturer's instructions or the calcium phosphate precipitation method, as previously described (17, 47). Briefly, 4×10^5 and 1×10^5 cells were plated on 60-mm and 6-well dishes, respectively, 24 h before transfection, and the media were changed to DMEM with 5% charcoal dextran-stripped serum (CSS) 1 h before transfection. Equal amounts of total DNA, including a reporter, indicated plasmids, and vector alone were individually transfected into each well. After 24 h of transfection, cells were treated with ligands for another 24 h. Cells were harvested and assayed for chloramphenicol transferase (CAT) or luciferase assays (Promega). pRL-SV40 and pCMV-β-gal were used for internal controls in luciferase and CAT assays, respectively. Data were represented as mean ± S.D. from three to six independent experiments.

Yeast Two-hybrid Assay—A pAS2-ARLBD plasmid comprised of the GAL4 DNA binding domain (DBD) fused with the ligand binding domain (LBD) of the AR was used as bait to test the interaction with different domains of ARA70, which were constructed in the pACT2 vector containing the GAL4 activation domain. The transformed yeast Y190 cells were selected for growth on plates with 20 mM 3-aminotriazole and serial concentrations of androgens but without histidine, leucine, or tryptophan. The liquid assay was performed as described (17).

Immunocytofluorescence Staining—COS-1 cells at 1×10^5 were seeded on 2-well Labtek II slides (Nalge) 24 h before transfection with 0.5 μg of AR and with or without 1.5 μg of full-length ARA70 (ARA70-FL) using FuGENE 6 transfection reagent (Roche Applied Science). After 12 h of transfection, cells were treated with 10 nM dihydrotestosterone (DHT) or ethanol. Immunostaining was performed using anti-AR polyclonal antibody (NH27) and/or anti-ARA70 mouse monoclonal antibody (CC70 3), followed by incubation with Texas red-conjugated goat anti-rabbit and/or fluorescein isothiocyanate-conjugated goat anti-mouse antibodies (ICN). After washes, slides were mounted with the mounting media containing DAPI for localization of nuclei.

Pulse Chase Assay—COS-1 cells were seeded in 100-mm dishes and transfected with the AR, with or without ARA70 as indicated for 3 h using *Superfect* (Qiagen), cultured in methionine/cysteine-deficient media for 3 h, and then subjected to pulse metabolic labeling with [^{35}S]methionine/cysteine for 30 min. After changing to the chase medium, the cells were harvested at the times indicated in the figure. Whole cell extracts were prepared by radioimmune precipitation assay buffer (150 mM NaCl, 50 mM Tris, 10% SDS, 0.5% sodium deoxylate (w/v), and 1% Nonidet P-40) and then immunoprecipitated with anti-AR antibody (NH27). The specificity of the immunoprecipitation was confirmed using preimmune serum as well as protein A-Sepharose beads alone (data not shown). The AR protein levels were visualized by PhosphorImager and quantitated by ImageQuant V.1.2 (Molecular Dynamics). The cells were also transfected with 40 ng of pRL-SV40 for transfection efficiency control. Relative AR amounts were normalized with the internal control.

Tissue Collection and Immunohistochemical Staining—Tissue specimens were collected from prostate cancer patients after obtaining approval from the Research Subject Review Board at the University of Rochester Medical Center. Tumor samples were classified as normal, benign prostatic hyperplasia (BPH), low-grade adenocarcinoma (Gleason pattern 1, 2, and 3), and high-grade adenocarcinoma (Gleason pattern 4 and 5). For immunohistochemical staining, 5-μm paraffin-embedded sections were deparaffinized, hydrated, and soaked with 3% hydrogen peroxide for 15 min, followed by blocking with 20% horse serum for 45 min. Sections were then incubated with mouse monoclonal ARA70 (CC70 No. 3) antibody (1:500) at 4 °C overnight, followed by incubation with horse biotinylated anti-mouse IgG (1:200) at room temperature for 40 min. Mouse immunoglobin was used as the negative control in place of the primary antibody. Note that primary and secondary antibodies were diluted in Tris-buffered saline containing 1% horse serum and stood at room temperature for at least 30 min before use. Finally, staining was visualized with Vectastain ABC reagent (Vector Laboratories) and peroxidase substrate DAB solution (Vector Laboratories) as instructed by the manufacturer. The sections were then counterstained with Gill's hematoxylin 2. The Mann-Whitney *U* test was used for analysis of ARA70 expression in human prostate cancer samples. For staining ARA70 in mouse testis, methods used were the same as described above, except that M.O.M.™ mouse Ig blocking reagent (Vector Laboratories) and M.O.M.™ biotinylated anti-mouse IgG were used to replace with blocking reagent and the secondary antibody, respectively.

LNCaP Xenograft in Nude Mice—LNCaP (3×10^7) cells mixed in Matrigel (BD Biosciences) were inoculated into the dorsal region of nude mice. At 11 weeks after cell inoculation, one group of mice ($n = 3$) was castrated, whereas another group ($n = 3$) underwent a sham operation. 6 weeks after castration or sham operation, xenografts of each group were harvested, fixed in 10% neutral buffered formalin, processed routinely, embedded in paraffin, and subjected to immunohistochemical staining with ARA70 antibodies.

RESULTS

Mapping the AR-interacting Domains of ARA70—To determine which domain(s) of ARA70 interact with the AR, we performed the yeast two-hybrid assay using pAS2-AR-LBD and pACT2 vectors containing different segments of ARA70 (Fig. 1*A*). As shown in Fig. 1*B*, ARA70N peptide (amino acids 1–401) and ARA70-N2 peptide (amino acids 176–401) can interact with the AR-LBD in the presence of 10 nM DHT. In contrast, three other ARA70 peptides, L*XX*LL motif-containing peptide (amino acids 90–99; *X*, any amino acid), ARA70-N1 (amino acids 1–175) and ARA70-C (amino acids 383–614) cannot interact with the AR-LBD. Using the mammalian two-hybrid system, our data further confirmed that ARA70-N2, but not ARA70-N1 or ARA70-C, can interact with the AR in an androgen-dependent manner (Fig. 1*C*). These data clearly demonstrate that ARA70-N2, lacking the consensus L*XX*LL motif, is essential for interaction with the AR-LBD in the presence of androgen, which is different from common coregulators, such as members of p160 family, SRC-1, TIF2/GRIP1, and p/CIP/AIB1/ACTR, that show a ligand-dependent interaction with SRs via the L*XX*LL motifs (48).

The FXXLF, but Not LXXLL, Motif in ARA70 Mediates the Interaction with AR—To further confirm that the L*XX*LL motif is dispensable for interaction with AR (42), we assessed the

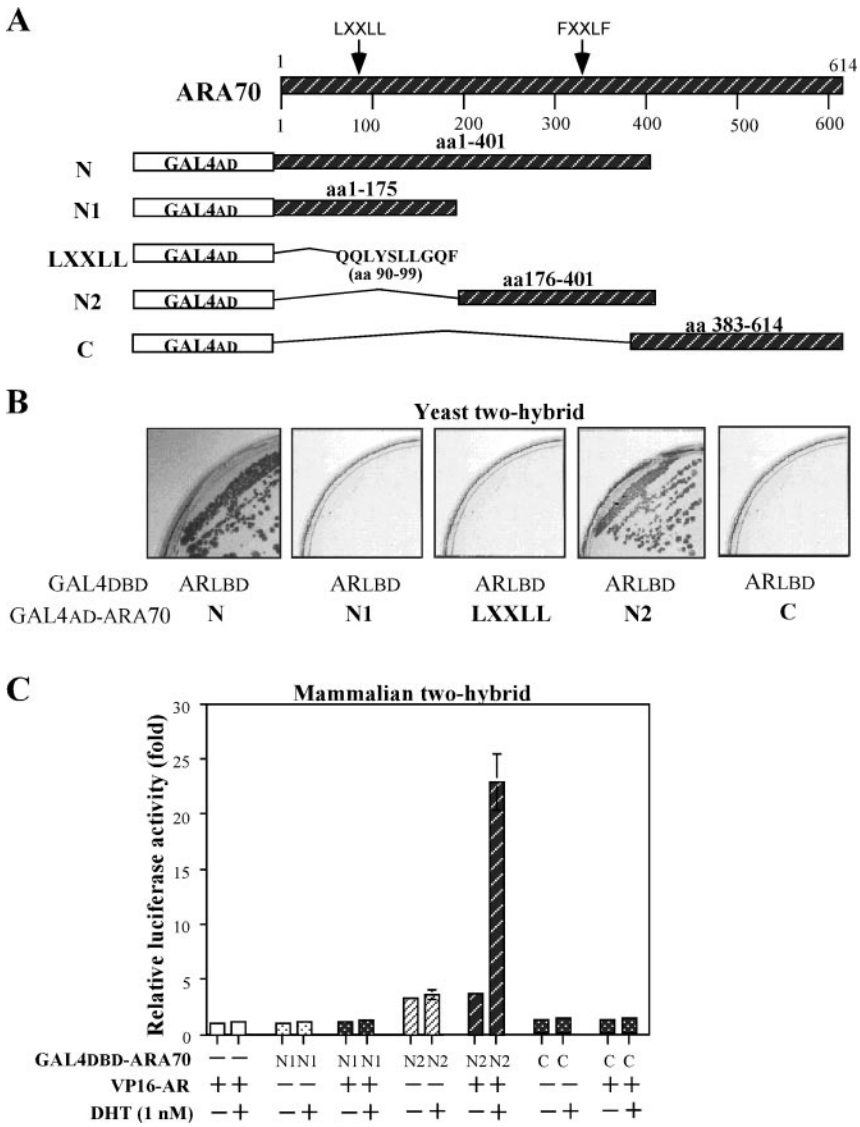

FIG. 1. **Mapping the AR-interacting domains of ARA70.** *A*, schematic diagram of the GAL4 activation domain-ARA70 fusion constructs used in the yeast two-hybrid assay. *B*, interaction of different domains/motifs of ARA70 with wild-type AR was assayed using the yeast Y190 strain with the plate nutritional selection. GAL4DBD-ARLBD, a fusion protein of the GAL4DBD fused with the AR peptide containing part of the DBD, the whole hinge region, and the LBD, was used as bait. The yeast cells were transformed with indicated constructs and selected on plates with 20 mM 3-aminotriazole and 10 nM DHT but without histidine, leucine, and tryptophan. The presence of yeast cells on the selection plates indicates that there is the positive interaction of ARLBD with ARA70-N and ARA70-N2 fragments. Data were reproducible in two independent experiments. *C*, mapping the AR-interacting domains of ARA70 by the mammalian two-hybrid assay. DU145 cells in 60-mm dishes were transiently transfected with 3 μg of each indicated plasmid and 3 μg pG5-Luc reporter by the calcium phosphate precipitation method for 24 h, and treated with 10 nM DHT for another 24 h. 40 ng of pRL-SV40 were used for internal control. Cells were then harvested for the luciferase assay. Results are representative of at least three independent experiments and are shown as mean ± S.D.

AR-interacting capacity of ARA70N-L*XX*AA, where the L*XX*LL motif was mutated to the L*XX*AA (Fig. 2*A*), in the mammalian two-hybrid system. As shown in Fig. 2*B*, there is no significant difference between ARA70N-L*XX*LL and -L*XX*AA interaction with the AR-LBD. Because ARA70 is also a coregulator of PPARγ (46), we tested if this mutation affects the ARA70-PPARγ interaction. Interestingly, ARA70N-L*XX*AA mutant showed a reduced degree of capacity to interact with PPARγ (Fig. 2*B*), suggesting that ARA70 functions as a coregulator of AR and PPARγ via distinct molecular mechanisms, where the L*XX*LL motif in ARA70 may play much more important roles for interaction with PPARγ than with AR.

Because our previous report (45) identified the F*XX*LF as one of the major androgen-dependent AR-interacting motifs using phage display screening system and Zhou *et al.* (42) demonstrated that the F*XX*LF motif within ARA70 is required for the androgen-dependent interaction with AR-LBD, we assessed whether the F*XX*LF motif in ARA70-N2 mediates AR-ARA70 interaction. Using the mammalian two-hybrid system, we found that GAL4-ARA70N interacts well with VP16-AR, whereas two mutants GAL4-ARA70N-A*XX*LF and -F*XX*AA lose the capacity to interact with AR (Fig. 2*C*). These results indicated that the F*XX*LF motif within the ARA70-N2 domain plays an essential role for the interaction between ARA70 and AR, which is consistent with the results in Fig. 1 showing that ARA70-N2 contains the AR-interacting domain.

Effect of Different Domains and the Role of the LXXLL and FXXLF Motifs of ARA70 on AR Transactivation—To delineate the functional domains of ARA70, the CAT assay was employed to determine the effect of various ARA70 fragments (Fig. 3*A*) on AR transactivation in DU145 cells. As shown in Fig. 3*B*, ARA70N and ARA70-FL, as well as their L*XX*AA mutants, showed an enhancement of AR transactivation, whereas neither ARA70-N1 nor ARA70-N2 could enhance AR transactivation. Because there is no significant difference between wild type and the L*XX*AA mutant of ARA70N or ARA70-FL on enhancing AR transactivation, these results may suggest that the L*XX*LL motif is dispensable for ARA70 function as an AR coactivator. This correlates with the interaction data (Fig. 2) and the previous report (42) showing that the L*XX*LL motif within ARA70-N1 domain is not required for the ARA70-AR interaction. However, ARA70-N1 is essential for the coactivator function of ARA70, because ARA70-N2 containing the AR-interacting motif alone cannot potentiate the AR transcriptional activity. Interestingly, ARA70N, containing both ARA70-N1 and -N2, shows stronger enhancement activity on AR than ARA70-FL, suggesting that ARA70-C may possess the activation inhibition domain. On the other hand, mutations on the F*XX*LF motif in ARA70N, which fails to interact with AR, results in the loss of coactivator function on the AR transactivation (Fig. 3*C*).

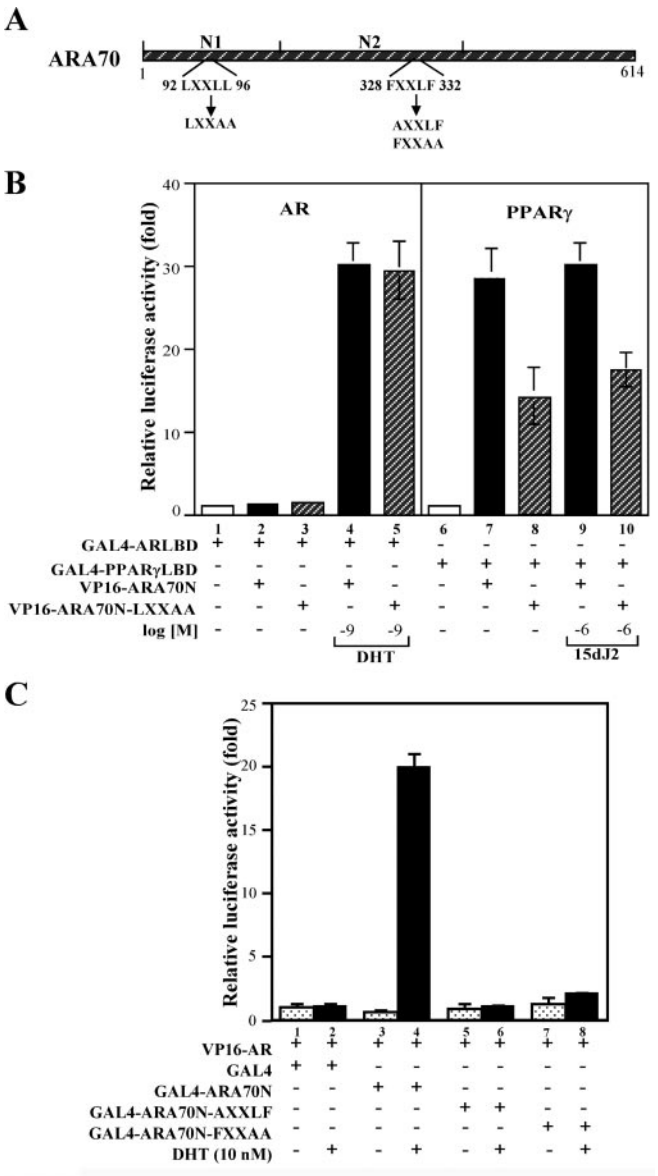

FIG. 2. **The F*XX*LF, but not L*XX*LL, motif in ARA70N is required for interaction with AR.** *A*, schematic diagram of the mutation sites on ARA70N generated by PCR. *B*, differential importance of the consensus L*XX*LL motif for ARA70N interaction with AR and PPARγ. DU145 cells in 60-mm dishes were transiently transfected with 3 μg of each indicated plasmid and 3 μg of pG5-Luc reporter by the calcium phosphate precipitation method for 24 h and treated with ligands for another 24 h. 40 ng of pRL-SV40 was used for internal control. Cells were then harvested for the luciferase assay. *C*, F*XX*LF motif in ARA70N is essential for the interaction with AR. Methods used are the same as described in *B*. Results are representative of at least three independent experiments and are shown as mean ± S.D.

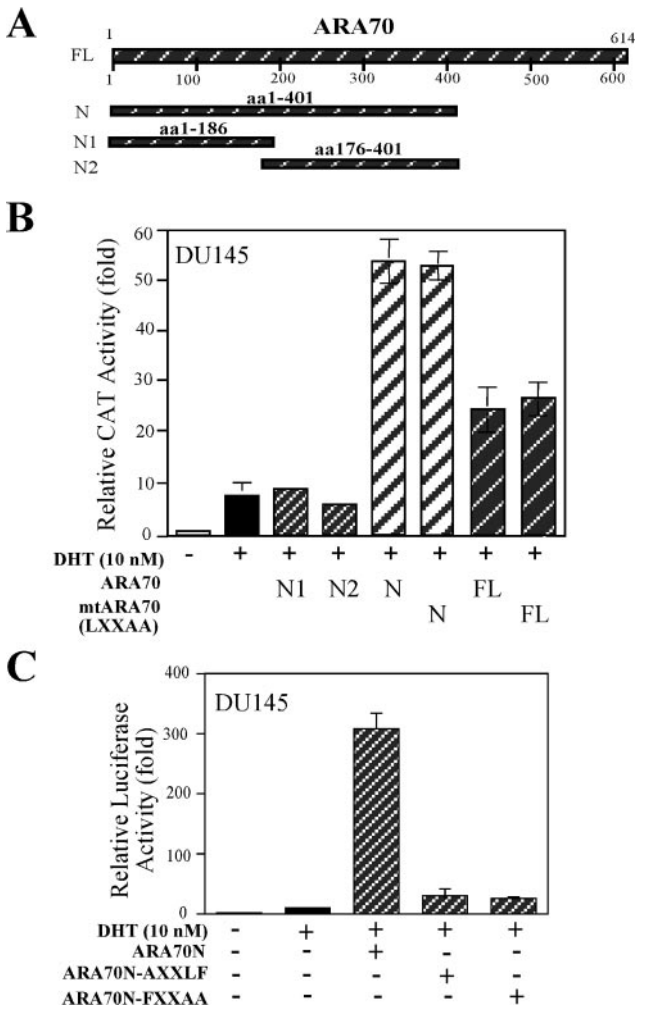

FIG. 3. **Effect of ARA70 domains/motifs on AR-mediated transactivation in prostate cancer cells.** *A*, schematic diagram of the constructs of pSG5-ARA70 fragments. *B*, ARA70- or ARA70N-enhanced AR transactivation is not mediated via the L*XX*LL motif. DU145 cells in 60-mm dishes were transiently transfected with pSG5-AR, MMTV-CAT reporter, and indicated constructs by the calcium phosphate precipitation method for 24 h and treated with 10 nM DHT for another 24 h. pCMV-β-gal was used for transfection efficiency. Cells were then harvested for the CAT assay. *C*, F*XX*FL motif is required for ARA70N to enhance the AR transactivation. DU145 cells in 60-mm dishes were transiently transfected with pSG5-AR, MMTV-Luc reporter, and indicated constructs by the calcium phosphate precipitation method for 24 h and treated with 10 nM DHT for another 24 h. pRL-SV40 was used for the internal control. Cells were then harvested for the luciferase assay. Results are representative of at least three independent experiments and are shown as mean ± S.D.

ARA70 Enhances AR Expression Level and Protein Stability—Although ARA70 has long been known as an AR coactivator, the molecular mechanism remains unclear. We first determined whether ARA70 can influence the AR expression level using the Western blot analysis. As shown in Fig. 4*A*, both ARA70-FL and ARA70N can increase the AR protein amount, while antisense ARA70 and TR4, another AR-interacting protein (49), show little influence on AR protein expression. Furthermore, to investigate whether the increase of AR expression by ARA70 is caused by the enhancement of AR protein stability, the pulse chase experiment was employed. As shown in Fig. 4*B*, in the absence of ARA70, AR protein was degraded gradually with a half-life of ~0.8 h. In the presence of ARA70, the half-life of AR was ~2.3 h. These results suggest that increasing AR expression by ARA70 is at least in part caused by the enhanced metabolic stability. In contrast, TR4 reduced the AR protein stability (AR half-life ~0.75 h in the presence of TR4, compared with ~0.9 h in the absence of TR4, Fig. 4*C*).

ARA70 Enhances AR Nuclear Staining—To explore if ARA70 influences the cellular distribution of AR, immunocytofluorescence staining assays were performed using AR (NH27) or ARA70 (CC70 No. 3) antibody. As shown in Fig. 5, the AR was mainly located in the cytoplasm in the absence of androgen (Fig. 5*A*) and moved into the nucleus after addition of 10 nM DHT (Fig. 5*B*). ARA70 was located mainly in the cytoplasm in the absence or presence of 10 nM DHT in COS-1 cells (Fig. 5, *C versus D*). Co-transfection of ARA70 and AR in the presence of 10 nM DHT enhanced the intensity of nuclear AR immunostaining, compared with that in the cells without ARA70 ex-

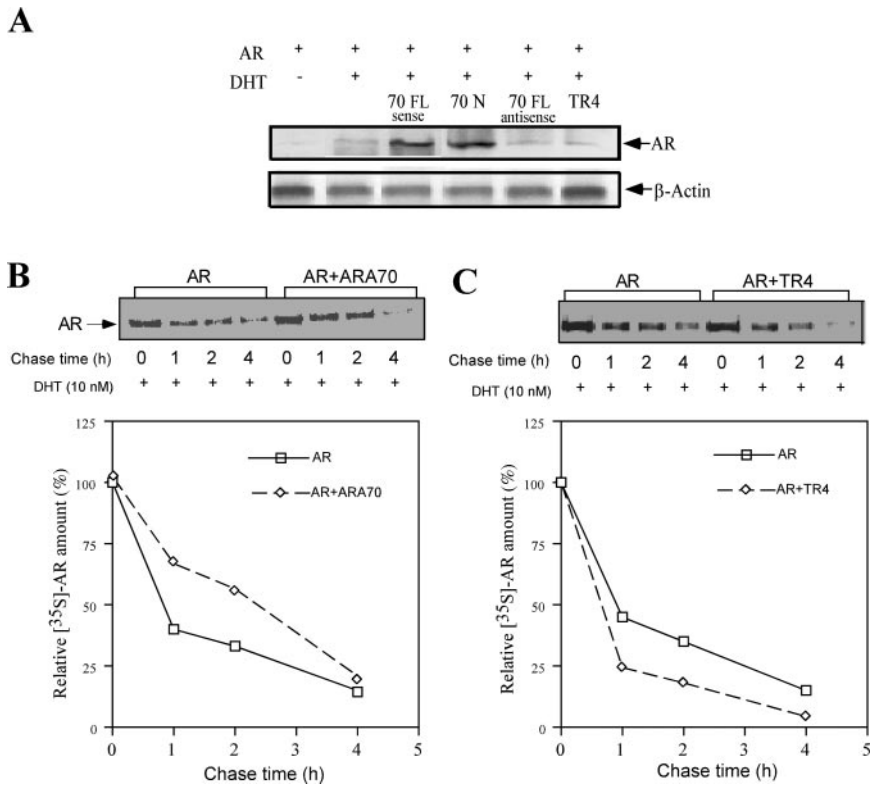

FIG. 4. **ARA70 enhances the expression level and the protein stability of AR.** *A*, COS-1 cells in 60-mm dishes were transfected with 5 μg of AR and 5 μg of indicated plasmids by the calcium phosphate precipitation method for 24 h, and treated with 10 nM DHT for another 24 h. Nuclear extracts were then prepared and 30 μg of nuclear extracts were subjected to Western blotting with polyclonal anti-AR and anti-β-actin antibodies. *B* and *C*, COS-1 cells in 100-mm dishes were transfected with 5 μg of AR and 5 μg of ARA70 (*B*) or TR4 (*C*) by SuperFect reagent and then subjected to a pulse chase assay using [^{35}S]methionine/cysteine labeling, as described under "Experimental Procedures." Cells were harvested at the indicated time for immunoprecipitation with a polyclonal anti-AR antibody (NH27). The AR protein levels were visualized by PhosphorImager and quantitated by ImageQuant V.1.2. The cells were also transfected with 40 ng of pRL-SV40 for transfection efficiency control. Relative AR amounts indicated in the *bottom panels* were normalized with the internal control.

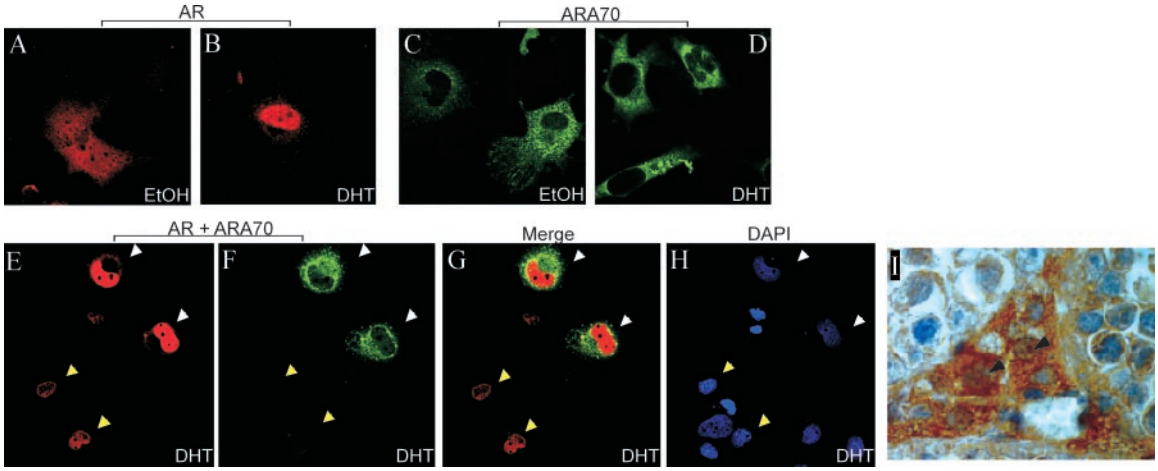

FIG. 5. **Cellular localization of AR and ARA70.** COS-1 cells were seeded on chamber slides and transfected with 0.5 μg of AR and/or 1.5 μg of full-length ARA70 using FuGENE 6 transfection reagent. After 24 h of transfection, cells were treated with 10 nM DHT or ethanol. Immunostaining was performed using the rabbit anti-AR polyclonal antibody (NH27) and/or mouse anti-ARA70 monoclonal antibody (CC70 No. 3), followed by Texas red-conjugated goat anti-rabbit and/or FITC-conjugated goat anti-mouse antibodies (ICN). The *red signal* represents the AR, and the *green signal* represents ARA70, as indicated. *Blue* DAPI staining shows the localization of nuclei. *A*, AR with ethanol; *B*, AR with DHT; *C*, ARA70 with ethanol; *D*, ARA70 with DHT; *E–H*, co-transfection of AR and ARA70. The cells expressing the AR only are indicated with *yellow arrows*, and the cells expressing both of AR and ARA70 are indicated with *white arrows*: *E*, AR staining; *F*, ARA70 staining; *G*, overlaying *E* and *F*; *H*, DAPI staining. EtOH, ethanol treatment. *I*, immunohistochemical analysis of ARA70 expression in testicular Leydig cells. Testes from mature male mice were paraffin-embedded, sectioned, and subjected to immunohistochemical staining with mouse ARA70 (CC70 3) antibody. Results indicate that ARA70 is expressed in the interstitial space between the seminiferous tubules. Leydig nuclei are indicated by *arrows*. Data are representative of at least three independent experiments. Original magnification, ×400.

pression (Fig. 5, *E–H*, *white arrows versus yellow arrows*). After scoring the AR staining intensity from 300 cells under a fluorescence microscope based on a scale of 1 (low) to 5 (high) and in the presence or absence of ARA70, we found that nuclear AR staining intensity was significantly higher ($p < 0.0005$) in the cells with ARA70 than without ARA70. The increased AR nuclear localization by ARA70 may contribute to the enhancement of AR transactivation. When staining the ARA70 in the AR-positive and androgen-responsive Leydig cells in the mouse testis, we found that ARA70 is expressed in both cytoplasm and nucleus, and mainly in the cytoplasm (Fig. 5*I*), which is in agreement with the previous report (50). Because Leydig cells are primarily involved in the production of testosterone (51), the cytosolic and nuclear localization of ARA70 shown in Fig. 5*I* is presumably in the presence of testosterone.

ARA70-N2 Inhibits AR Interaction with Coregulators, N- and C-terminal Interaction, and Transactivation—Because ARA70-N2 contains an AR-interacting motif but without coactivator function (Figs. 1–3), we further assessed if ARA70-N2 can be an inhibitor of AR transactivation by interrupting AR interaction with other coregulators and AR N- and C-terminal interaction. Using the mammalian two-hybrid system, we first found that

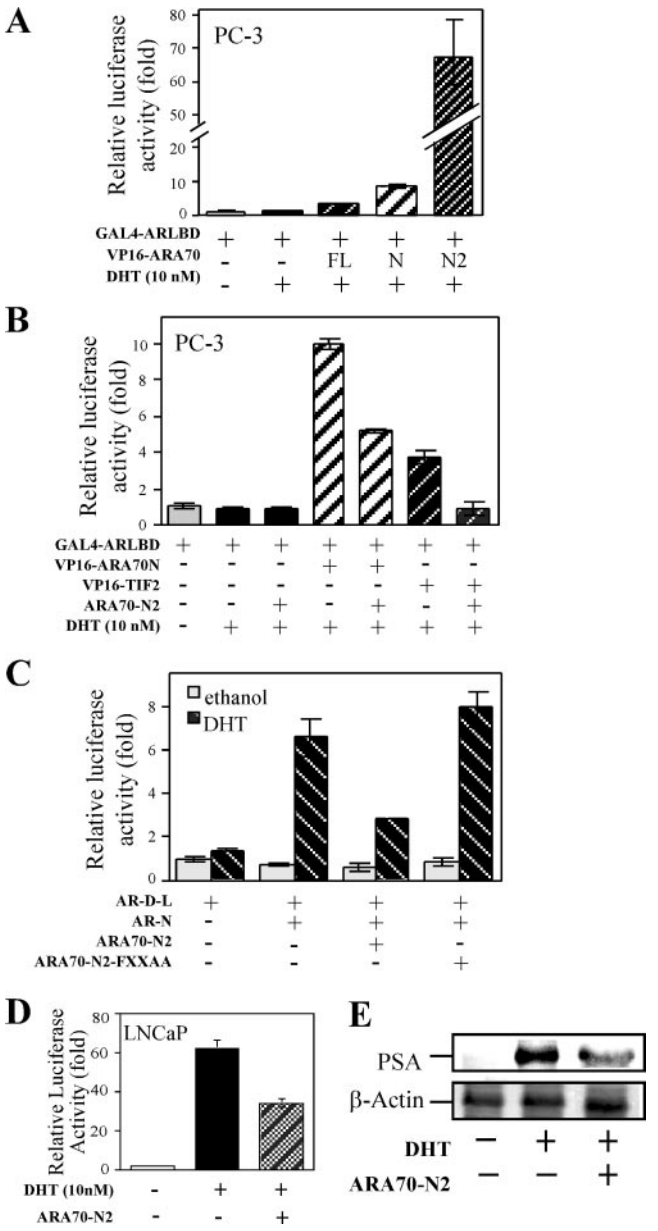

FIG. 6. **ARA70-N2 can serve as an inhibitor of AR transactivation.** *A*, ARA70-N2 has a stronger AR binding capacity than ARA70-FL and ARA70N in mammalian two-hybrid assay. PC-3 cells in 24-well dishes were transiently transfected with indicated plasmids and pG5-Luc reporter using SuperFect reagent for 24 h, and treated with 10 nM DHT for another 24 h. pRL-SV40 was used for internal control. Cells were then harvested for the luciferase assay. *B*, ARA70-N2 inhibits the interaction of AR with ARA70N and with TIF2. Methods used are the same as described in *Panel A*. *C*, ARA70-N2 inhibits the N- and C-terminal interaction of AR via the F*XX*LF motif. Methods used are the same as described in *Panel A*, except that the MMTV-Luc reporter, pCDNA3-FLAG-AR-DBD-LBD (AR-D-L, aa 507~919) and pCDNA3-FLAG-AR-N (AR-N, amino acids 1~556) were used. *D* and *E*, ARA70-N2 functions as an inhibitor to suppress the endogenous AR transactivation (*D*), and AR-mediated PSA expression (*E*) in LNCaP cells. 0.8 μg of ARA70-N2 and 0.2 of μg MMTV-Luc were transfected into LNCaP cells in the 24-well dishes for luciferase assay. 10 μg of ARA70-N2 were transfected into LNCaP cells in 100-mm dishes for Western blotting using anti-PSA and anti-β-actin antibodies. Transfections were performed using *Superfect* reagent and 24 h after transfection, cells were treated with 10 nM DHT for another 24 h. Results are representative of at least three independent experiments.

VP16-ARA70-N2 showed a much stronger induction of the pG5-luciferase reporter gene in the presence of the GAL4-AR-LBD, compared with VP16-ARA70-FL or -ARA70N, in PC-3 prostate cancer cells (Fig. 6*A*). This result indicates that ARA70-N2 possesses a much stronger AR binding capacity. Furthermore, ARA70-N2 was able to inhibit the association of GAL4-AR-LBD with VP16-ARA70N and another coregulator VP16-TIF2 that binds AR via the L*XX*LL motif (52) (Fig. 6*B*). These data suggest that ARA70-N2, with higher AR binding capacity, is capable of competing with other coregulators to interact with liganded AR-LBD. Because the androgen-induced N- and C-terminal interaction via the F*XX*LF motif in the N terminus and the AF2 domain in the LBD is essential for AR transactivation (53), we determined whether ARA70-N2 can inhibit AR transactivation through competing with the AR N-terminal F*XX*FL motif to interact with AR-LBD. As shown in Fig. 6*C*, DHT treatment induced the interaction between the N and C termini of AR, and ARA70-N2 indeed suppressed this interaction. In contrast, ARA70-N2-F*XX*AA mutant had no influence on the AR N- and C-terminal interaction. These results suggest that the suppression of AR transactivation by ARA70-N2 involves not only the blockade of AR interaction with coregulators, but also the inhibition of AR N- and C-terminal interaction. Fig. 6, *D* and *E* further demonstrate that ARA70-N2 can repress AR reporter and endogenous AR target gene, prostate-specific antigen (PSA), expression (Fig. 6*E*) in androgen-responsive LNCaP prostate cancer cells. Together, these results indicate that ARA70-N2 can serve as an inhibitor to suppress *in vivo* AR transactivation.

TABLE I

The percentage of the ARA70 immunoreactive specimens is significantly higher in prostate cancer tissues than in benign tissues

Tissue samples were collected from 80 prostate cancer patients. Results were recorded as positive (more than 5% cells positive) or negative (less than 5% cells positive).

Type		ARA70 expression				
		n	Positive	Negative	Positivity	p^a
					%	
Benign	Normal	44	35	9	79.55	
	BPH	69	38	31	55.07	
	Total	113	73	40	64.60	
Neoplastic[b]	Low grade	66	59	7	89.39	<0.0005
	High grade	43	41	2	95.35	<0.0001
	Total	109	100	9	91.74	<0.0001

[a] Using Fisher's exact test, statistically significant difference in ARA70 positivity is observed ($p < 0.05$), when compared with that in total benign tissues.

[b] Neoplastic prostate tissues are classified as follows: Gleason pattern 1, 2, and 3 are defined as low grade and Gleason pattern 4 and 5 are defined as high grade.

The Positivity of ARA70 Is Significantly Higher in Prostate Cancer Tissues Compared with Benign Tissues—To determine whether ARA70 is associated with the prostate cancer development, the ARA70 protein expression was examined in a number of the prostate samples that include various stages of prostate tumors collected from 80 patients. Using anti-ARA70 monoclonal antibody for immunohistochemical staining, we found that the percentage of ARA70 immunoreactive specimens significantly increased from 64.60% (73 of 113 samples) in benign prostate tissues to 91.74% (100 of 109 samples) in neoplastic prostate tissues ($p < 0.0001$, Table I). The significant increase in ARA70 positivity in the malignant prostate tissues strengthens the hypothesis that ARA70 plays an important role in the prostate cancer development.

ARA70 Expression Is Increased in the High Grade Prostate Tumors and in the Hormone-refractory Prostate Cancer Xenograft—To further explore the biological relevance of ARA70 and prostate cancer, we evaluated the ARA70 expression level in different stages of prostate cancer tissues. Using immunohistochemical staining, we found that ARA70 expression was increased in prostate tumors as compared with normal or benign prostate tissues adjacent to the tumors (Fig. 7*A*). In ad-

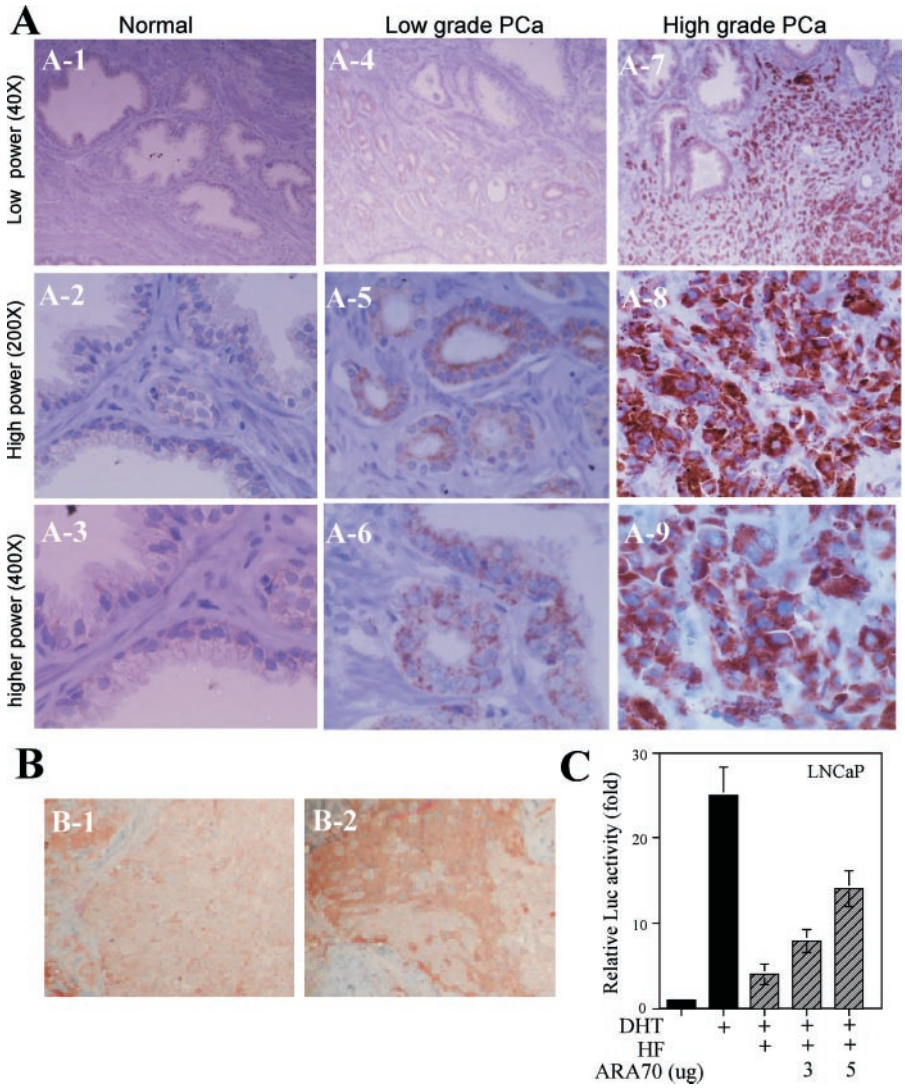

FIG. 7. **ARA70 expression is increased in the higher grade of prostate cancer and in the hormone-refractory LNCaP xenograft in nude mice, and the increased expression of ARA70 can promote AR activity in the presence of HF.** *A*, immunohistochemical staining of ARA70 in the prostate tumors. Prostate cancer tissues with adjacent normal areas were collected, graded by pathologists, and processed for immunohistochemical staining with ARA70 antibody. ARA70 expression is increased in the higher grade of prostate cancer tissues (*A-7–9*), compared with the lower grade samples (*A-4–6*) and adjacent normal tissues (*A-1–3*). Original magnification: ×40, ×200, and ×400, as indicated. *B*, ARA70 expression is higher in the LNCaP xenograft in castrated nude mice (*B-2*) than in non-castrated nude mice (*B-1*). Xenografts were paraffin-embedded and processed for immunohistochemical staining with ARA70 antibody. Original magnification: ×20. *C*, LNCaP cells were transfected with ARE4-Luc reporter and increasing amounts of ARA70 plasmids using SuperFect reagent for 24 h, followed by treatments with DHT and/or HF for another 24 h as indicated in the figure. Cells were then harvested for luciferase assay. Results are representative of at least three independent experiments and are shown as mean ± S.D.

dition, the ARA70 expression is also increased in LNCaP xenograft in castrated nude mice compared with non-castrated nude mice (Fig. 7*B*). Although the increased expression of ARA70 may not occur in all high grade prostate cancer cases (54), our results from Fig. 7, *A* and *B* suggest that ARA70 expression is, at least in some cases, induced at the later stage of prostate cancer after androgen ablation therapy with surgical/chemical castration and/or anti-androgen (HF or casodex) treatment. Because higher expression of ARA70 can enhance the androgenic activity of HF on AR (Fig. 7*C*), it is likely that the increased ARA70 expression in the later stage of prostate cancer (Fig. 7, *A* and *B*) may promote the AR transactivation in the patients treated with HF. HF withdrawal syndrome is a symptom that occurs in many prostate cancer patients at the later stage where HF conversely enhances AR activity as an agonist, and discontinuation of HF treatment results in significant reduction of PSA expression, often associated with clinical improvement (55). While the molecular basis for the HF withdrawal syndrome is not fully understood, our results may suggest that increased expression of ARA70 in high grade prostate cancer may partly confer the development of this syndrome.

ARA70 Expression Is Increased in Prostate Cancer Cells Cultured in the Androgen-deficient Condition, and ARA70-N2 Can Suppress HF-activated AR Transactivation—Using Western blot analysis, we found that the hormone-refractory CWR22R prostate cancer cells expressed a higher degree of ARA70 protein, when cultured in the CSS media for 6 days (Fig. 8*A*). Also, LNCaP cells cultured in CSS media for 15 weeks (hormone refractory LNCaP, that mimics the prostate cancer at the hormone refractory stage) demonstrated an increased ARA70 mRNA expression, as compared with the cells cultured in normal media (Fig. 8*B*). A missense mutation (T877A) on the *AR* gene is the first mutation reported that leads to androgen independence, is frequently found in cases of androgen-independent prostate cancer (56), and allows HF to function as an agonist to enhance AR transactivation, which is a phenomenon found in HF withdrawal syndrome (44). Therefore, it is of interest to determine whether ARA70-N2 can serve as a repressor to inhibit the HF-enhanced AR transactivation in the hormone-refractory LNCaP cells that contain the AR with the T877A mutation. As shown in Fig. 8*C*, ARA70-N2, but not ARA70-N1, could indeed suppress HF-activated AR activation in a reporter gene assay.

DISCUSSION

AR plays essential roles in the proliferation of the prostate gland and the prostate cancer. In the later stages of prostate cancer, more than 80% of prostate cancer tissues remain positive for AR staining (57, 58), suggesting that AR may play a role for the progression of the prostate cancer. Understanding the molecular mechanisms of AR is therefore of biological and clinical importance. The AR activity in prostate cancer has been known to be influenced by many factors, including AR

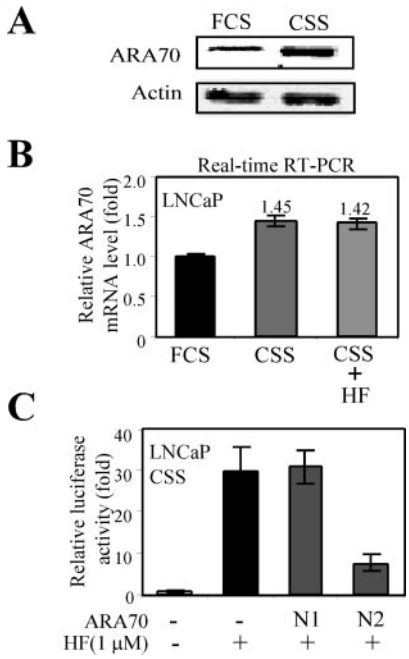

FIG. 8. **ARA70 expression is increased in the prostate cancer cells cultured in the androgen-deficient CSS, and ARA70-N2 can inhibit AR transactivation activated by HF in these cells.** *A*, CWR22R prostate cancer cells were cultured in RPMI 1640 media with normal FCS or CSS for 6 days. 100 μg of total protein from each cell lysate was subjected to Western blotting with anti-ARA70 and anti-β-actin antibodies. *B*, LNCaP cells were cultured in RPMI media containing normal FCS, CSS, or CSS plus 1 μM HF for 15 weeks. Total RNAs were harvested, and ARA70 mRNA expression levels were determined by real-time RT-PCR using a pair of primers: 5′-CAAGACTGACTCCTGTACCAACTG-3′ and 5′-AGCCTCCTTCTCACAATTCTCATC-3′. Relative amounts of ARA70 mRNA were normalized with the β-actin mRNA levels. *C*, LNCaP cells, long term cultured in CSS media, were transfected with MMTV-luc and indicated plasmids using SuperFect reagent for 24 h, followed by treatment with 1 μM HF for another 24 h. Cells were then harvested for the luciferase assay. Results are representative of at least three independent experiments and are shown as mean ± S.D.

gene amplification, AR mutations that change the hormone specificity/sensitivity, overactivated growth factor/kinase pathways, and differential levels of AR coregulators (59, 60). In the present study, we investigated the molecular mechanism underlying the coactivator function of ARA70 by first defining the AR-interacting domain of ARA70, which is located at the F*XX*LF motif, but not the L*XX*LL motif. The L*XX*LL motif has been identified as the signature motif for p160 coregulators to interact with SRs (28, 48). It has been well documented that the removal of the L*XX*LL motif can abolish the interaction between p160 coregulators and SRs. In contrast, our results indicate that this L*XX*LL motif is not essential for ARA70 to interact with the AR. In addition, sequence analysis revealed that ARA70 is lacking other common coregulator motifs, such as the basic helix-loop-helix domain, and the Per-AhR-Sim, that are shared by the p160 coregulator family, including SRC-1, TIF2/GRIP1, and AIB1/P/CIP/RAC3/ACTR/SRC3 (22–28). Nevertheless, whereas the L*XX*LL motif is dispensable for the interaction with the AR, it is important for interacting with the non-classical nuclear receptor PPARγ (Fig. 2) and estrogen receptor (data not shown). These results suggest that ARA70 may utilize distinct mechanisms to interact with and promote the activity of different nuclear receptors.

SRs function as transcription factors to regulate the expression of their target genes in the nucleus. Before ligand binding, some SRs are located in the cytosol (61) and are associated with HSPs. HSPs behave as protein chaperones in maintaining the proper conformation of SRs, thereby assisting in their consequent activation (5–7). It is anticipated that other cytosolic proteins may also contribute to the proper functioning of the receptors, including cytosolic mediators of signal transduction phosphorylation cascades, transportation, anchoring, ubiquination, or degradation of SRs. Overall, these cytosolic regulations may subsequently affect SR transactivation occurring in the nucleus.

The immunostaining results show that ARA70 is mainly expressed in the cytosol of testicular Leydig cells and prostate epithelial cells in the prostate cancer specimens. Also, ectopically expressed full length ARA70 was stained mainly in the cytosol of COS-1 cells (Fig. 5, *A–H*). This raises interesting questions of how a cytosolic ARA70 has the capacity to enhance AR transactivation. One possible mechanism could be to stabilize or increase the activated form of the AR, by either slowing down the degradation rate or increasing AR protein synthesis. Another possibility may involve a conformational change of the cytosolic AR so that it may bind to and/or retain androgen more easily, possibly resulting in a faster nuclear translocation. The results from pulse chase labeling indicate that AR protein is more stable by the co-transfection of ARA70 during the first 4 h. The metabolic stabilization of AR and/or increasing AR protein amount in the presence of ARA70 was also confirmed by Western blot analysis and semiquantitation of nuclear AR immunostaining using fluorescence microscopy. Other reports have also demonstrated that cytosolic proteins or even membrane-bound proteins, such as β-catenin and caveolin, can function as coactivators to enhance AR transactivation (39, 62), though the detailed mechanism underlying these phenomena remains to be elucidated.

It has been found that SR coregulators may exist as different isoforms to function as receptor coregulators. For example, SRC-1a and SRC-1e possess different capacities to regulate SR activity (63, 64). Our data also indicate that ARA70N, a peptide lacking the C-terminal domain of ARA70, has better coregulator activity. Furthermore, whereas the distribution of cytosolic ARA70 was not influenced by addition of the AR and 10 nM DHT, ARA70N was translocated to the nucleus with the AR in the presence of androgen (data not shown). This distinct cellular distribution may explain why ARA70N has better coactivator activity. However, whether there is one or some of ARA70 splicing isoforms that share the function and structure with ARA70N in the prostate cells needs to be further investigated.

In addition to the significant association of the ARA70 positivity with prostate cancer development (Table I), results from Figs. 7 and 8 raise a new possibility to explain how prostate tumors develop into the HF withdrawal syndrome, at least in some cases. That is, ARA70 expression is increased in hormone-refractory prostate cancer cells at protein and mRNA levels, which may promote the androgenic activity of HF to enhance the AR activity and PSA expression. Because ARA70-N2 can block both androgen- and HF-activated AR transactivation by competing with other coregulators to bind to AR, using an inhibitory peptide like ARA70-N2 or compounds possessing the similar inhibition function may become an alternative therapeutic strategy against prostate cancer, when anti-androgen treatment fails.

In summary, ARA70 modulates the AR activity via distinct domains and multiple mechanisms. Because of the biological relevance of ARA70 in the prostate cancer progression proposed in this study, dissection of the detailed mechanisms of how ARA70 can influence AR activity may provide us a better opportunity to battle prostate cancer.

Acknowledgments—We thank Hinrich Gronemeyer for providing plasmids and Karen Wolf for manuscript preparation. We are grateful

to Patricia A. Bourne and Jorge L. Yao for tissue collections, immunohistochemistry, and data analysis.

REFERENCES

1. Chang, C. S., Kokontis, J., and Liao, S. T. (1988) *Proc. Natl. Acad. Sci. U. S. A.* **85,** 7211–7215
2. Chang, C. S., Kokontis, J., and Liao, S. T. (1988) *Science* **240,** 324–326
3. Chang, C., Saltzman, A., Yeh, S., Young, W., Keller, E., Lee, H. J., Wang, C., and Mizokami, A. (1995) *Crit. Rev. Eukaryot. Gene Expr.* **5,** 97–125
4. Tsai, M. J., and O'Malley, B. W. (1994) *Annu. Rev. Biochem.* **63,** 451–486
5. Rajapandi, T., Greene, L. E., and Eisenberg, E. (2000) *J. Biol. Chem.* **275,** 22597–22604
6. Pratt, W. B., Czar, M. J., Stancato, L. F., and Owens, J. K. (1993) *J. Steroid Biochem. Mol. Biol.* **46,** 269–279
7. Pratt, W. B., and Toft, D. O. (1997) *Endocr. Rev.* **18,** 306–360
8. Chen, S., and Smith, D. F. (1998) *J. Biol. Chem.* **273,** 35194–35200
9. Fliss, A. E., Rao, J., Melville, M. W., Cheetham, M. E., and Caplan, A. J. (1999) *J. Biol. Chem.* **274,** 34045–34052
10. Fang, Y., Fliss, A. E., Robins, D. M., and Caplan, A. J. (1996) *J. Biol. Chem.* **271,** 28697–28702
11. Sadovsky, Y., Webb, P., Lopez, G., Baxter, J. D., Fitzpatrick, P. M., Gizang-Ginsberg, E., Cavailles, V., Parker, M. G., and Kushner, P. J. (1995) *Mol. Cell. Biol.* **15,** 1554–1563
12. Baniahmad, A., Ha, I., Reinberg, D., Tsai, S., Tsai, M. J., and O'Malley, B. W. (1993) *Proc. Natl. Acad. Sci. U. S. A.* **90,** 8832–8836
13. McEwan, I. J., and Gustafsson, J. (1997) *Proc. Natl. Acad. Sci. U. S. A.* **94,** 8485–8490
14. Lee, D. K., Duan, H. O., and Chang, C. (2000) *J. Biol. Chem.* **275,** 9308–9313
15. Dynlacht, B. D., Hoey, T., and Tjian, R. (1991) *Cell* **66,** 563–576
16. Pugh, B. F., and Tjian, R. (1990) *Cell* **61,** 1187–1197
17. Yeh, S., and Chang, C. (1996) *Proc. Natl. Acad. Sci. U. S. A.* **93,** 5517–5521
18. Fujimoto, N., Yeh, S., Kang, H. Y., Inui, S., Chang, H. C., Mizokami, A., and Chang, C. (1999) *J. Biol. Chem.* **274,** 8316–8321
19. Kang, H. Y., Yeh, S., Fujimoto, N., and Chang, C. (1999) *J. Biol. Chem.* **274,** 8570–8576
20. Hsiao, P. W., and Chang, C. (1999) *J. Biol. Chem.* **274,** 22373–22379
21. Hsiao, P. W., Lin, D. L., Nakao, R., and Chang, C. (1999) *J. Biol. Chem.* **274,** 20229–20234
22. Onate, S. A., Tsai, S. Y., Tsai, M. J., and O'Malley, B. W. (1995) *Science* **270,** 1354–1357
23. Hong, H., Kohli, K., Trivedi, A., Johnson, D. L., and Stallcup, M. R. (1996) *Proc. Natl. Acad. Sci. U. S. A.* **93,** 4948–4952
24. Voegel, J. J., Heine, M. J., Zechel, C., Chambon, P., and Gronemeyer, H. (1996) *EMBO J.* **15,** 3667–3675
25. Anzick, S. L., Kononen, J., Walker, R. L., Azorsa, D. O., Tanner, M. M., Guan, X. Y., Sauter, G., Kallioniemi, O. P., Trent, J. M., and Meltzer, P. S. (1997) *Science* **277,** 965–968
26. Chen, H., Lin, R. J., Schiltz, R. L., Chakravarti, D., Nash, A., Nagy, L., Privalsky, M. L., Nakatani, Y., and Evans, R. M. (1997) *Cell* **90,** 569–580
27. Li, H., Gomes, P. J., and Chen, J. D. (1997) *Proc. Natl. Acad. Sci. U. S. A.* **94,** 8479–8484
28. Torchia, J., Rose, D. W., Inostroza, J., Kamei, Y., Westin, S., Glass, C. K., and Rosenfeld, M. G. (1997) *Nature* **387,** 677–684
29. Smith, C. L., Onate, S. A., Tsai, M. J., and O'Malley, B. W. (1996) *Proc. Natl. Acad. Sci. U. S. A.* **93,** 8884–8888
30. Yeh, S., Miyamoto, H., Nishimura, K., Kang, H., Ludlow, J., Hsiao, P., Wang, C., Su, C., and Chang, C. (1998) *Biochem. Biophys. Res. Commun.* **248,** 361–367
31. Yeh, S., Hu, Y. C., Rahman, M., Lin, H. K., Hsu, C. L., Ting, H. J., Kang, H. Y., and Chang, C. (2000) *Proc. Natl. Acad. Sci. U. S. A.* **97,** 11256–11261
32. Ogryzko, V. V., Schiltz, R. L., Russanova, V., Howard, B. H., and Nakatani, Y. (1996) *Cell* **87,** 953–959
33. Spencer, T. E., Jenster, G., Burcin, M. M., Allis, C. D., Zhou, J., Mizzen, C. A., McKenna, N. J., Onate, S. A., Tsai, S. Y., Tsai, M. J., and O'Malley, B. W. (1997) *Nature* **389,** 194–198
34. Yeh, S., Miyamoto, H., Shima, H., and Chang, C. (1998) *Proc. Natl. Acad. Sci. U. S. A.* **95,** 5527–5532
35. Yeh, S., Lin, H. K., Kang, H. Y., Thin, T. H., Lin, M. F., and Chang, C. (1999) *Proc. Natl. Acad. Sci. U. S. A.* **96,** 5458–5463
36. Miyamoto, H., Yeh, S., Wilding, G., and Chang, C. (1998) *Proc. Natl. Acad. Sci. U. S. A.* **95,** 7379–7384
37. Han, G., Foster, B. A., Mistry, S., Buchanan, G., Harris, J. M., Tilley, W. D., and Greenberg, N. M. (2001) *J. Biol. Chem.* **276,** 11204–11213
38. Kemppainen, J. A., Lane, M. V., Sar, M., and Wilson, E. M. (1992) *J. Biol. Chem.* **267,** 968–974
39. Truica, C. I., Byers, S., and Gelmann, E. P. (2000) *Cancer Res.* **60,** 4709–4713
40. Agoulnik, I., Stenoien, D., Mancini, M. A., and Weigel, N. (2000) *Keystone Symposium: Nuclear Receptor Superfamily, Steamboat Springs, April 2000*, Bristol-Myers Squibb Pharmaceutical Research Institute and the Director's Sponsor Fund, Steamboat Springs, CO
41. Gregory, C. W., Hamil, K. G., Kim, D., Hall, S. H., Pretlow, T. G., Mohler, J. L., and French, F. S. (1998) *Cancer Res.* **58,** 5718–5724
42. Zhou, Z. X., He, B., Hall, S. H., Wilson, E. M., and French, F. S. (2002) *Mol. Endocrinol.* **16,** 287–300
43. Mitchell, S. H., Zhu, W., and Young, C. Y. (1999) *Cancer Res.* **59,** 5892–5895
44. Rahman, M. M., Miyamoto, H., Takatera, H., Yeh, S., Altuwaijri, S., and Chang, C. (2003) *J. Biol. Chem.* **278,** 19619–19626
45. Hsu, C. L., Chen, Y. L., Yeh, S., Ting, H. J., Hu, Y. C., Lin, H., Wang, X., and Chang, C. (2003) *J. Biol. Chem.* **278,** 23691–23698
46. Heinlein, C. A., Ting, H. J., Yeh, S., and Chang, C. (1999) *J. Biol. Chem.* **274,** 16147–16152
47. Hu, Y. C., Shyr, C. R., Che, W., Mu, X. M., Kim, E., and Chang, C. (2002) *J. Biol. Chem.* **277,** 33571–33579
48. Heery, D. M., Kalkhoven, E., Hoare, S., and Parker, M. G. (1997) *Nature* **387,** 733–736
49. Lee, Y. F., Shyr, C. R., Thin, T. H., Lin, W. J., and Chang, C. (1999) *Proc. Natl. Acad. Sci. U. S. A.* **96,** 14724–14729
50. Thin, T. H., Kim, E., Yeh, S., Sampson, E. R., Chen, Y. T., Collins, L. L., Basavappa, R., and Chang, C. (2002) *J. Biol. Chem.* **277,** 36499–36508
51. Payne, A. H. (1990) *Biol. Reprod.* **42,** 399–404
52. He, B., Minges, J. T., Lee, L. W., and Wilson, E. M. (2002) *J. Biol. Chem.* **277,** 10226–10235
53. He, B., Bowen, N. T., Minges, J. T., and Wilson, E. M. (2001) *J. Biol. Chem.* **276,** 42293–42301
54. Li, P., Yu, X., Ge, K., Melamed, J., Roeder, R. G., and Wang, Z. (2002) *Am. J. Pathol.* **161,** 1467–1474
55. Yeh, S., Miyamoto, H., and Chang, C. (1997) *Lancet* **349,** 852
56. Brinkmann, A. O., and Trapman, J. (2000) *Nat. Med.* **6,** 628–629
57. Culig, Z. (2003) *Urology* **62,** 21–26
58. van der Kwast, T. H., Schalken, J., Ruizeveld de Winter, J. A., van Vroonhoven, C. C., Mulder, E., Boersma, W., and Trapman, J. (1991) *Int. J. Cancer* **48,** 189–193
59. Heinlein, C. A., and Chang, C. (2002) *Endocr. Rev.* **23,** 175–200
60. Heinlein, C. A., and Chang, C. (2004) *Endocr. Rev.* **25,** 276–308
61. McNally, J. G., Muller, W. G., Walker, D., Wolford, R., and Hager, G. L. (2000) *Science* **287,** 1262–1265
62. Lu, M. L., Schneider, M. C., Zheng, Y., Zhang, X., and Richie, J. P. (2001) *J. Biol. Chem.* **276,** 13442–13451
63. Hayashi, Y., Ohmori, S., Ito, T., and Seo, H. (1997) *Biochem. Biophys. Res. Commun.* **236,** 83–87
64. Kalkhoven, E., Valentine, J. E., Heery, D. M., and Parker, M. G. (1998) *EMBO J.* **17,** 232–243